



# ANALYSIS OF MHD FLOW AND HEAT TRANSFER OF LAMINAR FLOW BETWEEN POROUS DISKS

V. S. Sampath Kumar<sup>a</sup>, N. P. Pai<sup>a,†</sup>, B. Devaki<sup>a</sup>

<sup>a</sup> Manipal Institute of Technology, Manipal Academy of Higher Education, Manipal, Karnataka, 576104, India

## ABSTRACT

A study is carried out for the two dimensional laminar flow of conducting fluid in presence of magnetic field. The governing non-linear equations of motion are transformed in to dimensionless form. A solution is obtained by homotopy perturbation method and it is valid for moderately large Reynolds numbers for injection at the wall. Also an efficient algorithm based finite difference scheme is developed to solve the reduced coupled ordinary differential equations with necessary boundary conditions. The effects of Reynolds number, the magnetic parameter and the Prandtl number on flow velocity and temperature distribution is analysed by both the methods and results agree well with previous work for special cases. It is observed that overall effect of magnetic field is same as Hartmann flow. Further the analysis predicts that the heat transfer at the surface of the disks increases with increase in Reynolds number, magnetic parameter and Prandtl number. The shear stress at the wall decreases with increase in injection, whereas increase with increase in magnetic parameter. The study of such phenomenon is beneficial in the industry for thermal control in polymeric processing.

**Keywords:** Navier-Stokes equations; Laminar flow; Incompressible flow; Non-linear differential equations; Homotopy Perturbation method; Finite Difference Method

## 1. INTRODUCTION

The flow of a conducting fluid between two porous disks is of practical importance in lubrication theory, such type of flows have lot of importance and applications in mechanical and manufacturing process, magnetic and storage devices (disk drives), gas engines, crystal growth process and bio-mechanics. MHD effects are used for power generators, light-ion-beam confinements and space crafts. Many authors contributed their efforts to understand these types of problems. The problem was first studied by Batchelor (Batchelor (1967)), who extended the study of Von Karman (Karman (2021)) for a flow over a single disk. Study about flow between rotating disks is done by many authors in 1960s (Lance and Rogers (1962), Root and Lewellen (1966)). The similar type of study with slight modification in the model in which one disk is rotating and one disk is stationary is done by Mellor (Mellor *et al.* (1968)). In 1979 Wang (Wang and Watson (1979)) and his associates further developed these models with suction or injection by considering the porous disks with rotation. The first MHD analysis about these type of models done by Srivastava and his associates in 1961 (Srivastava and Sharma (1961)). Later many authors contributed the better analysis in MHD in this type models (Stephenson (1969), Chandrasekhara and Rudriah (1971a), Chandrasekhara and Rudriah (1971b)). Further the problem was analysed by Stewartson (Stewartson (1953)) who found perturbation solution.

A recent study of this kind of problems are done by Si Xinhui (Xinhui *et al.* (2012)) in 2012, authors used homotopy analysis method for laminar flow and heat transfer of viscous fluid between contracting rotating

disks. In 2019 Naresh kumar and his associates (Raju *et al.* (2019)) studied the heat and mass transfer analysis of MHD couple stress fluid flow through contracting or expanding porous pipes. P Sibanda (Sibanda and Makinde (2012)) and his associates investigate the hydromagnetic steady flow and heat transfer characteristics of an incompressible viscous electrically conducting fluid past a rotating disk in a porous medium with ohmic heating, Hall current and viscous dissipation. Many authors studied this type of models under different conditions and these articles can be found in (Raju *et al.* (2019), Nazir and Mahmood (2011), Osalusi *et al.* (2007), Gu *et al.* (2020), Abed *et al.* (2020), Tufail *et al.* (2020), Gadamsetty *et al.* (2020)).

Solving these type of models through existing mathematical tools are also really challenging for the researcher, due to non-linear nature of the equations obtaining analytical solution is not possible in most of the cases, hence the most of the researchers have used numerical methods to solve this type of problems (Bujurke *et al.* (1995), Sampath and Pai (2019b), Sampath and Pai (2019a)), but numerical methods having their own demerits and most of the time getting solution to this kind of problems is a tedious job to the researchers. However, this class of problems are efficiently solved through semi analytical methods. One such method is homotopy perturbation method (HPM). HPM first proposed by Ji-Huan He in 1998 (He. (2006)). HPM is the combination of traditional perturbation method and homotopy in topology. Many authors used this method to solve different class of problems (Gupta *et al.* (2013), Abbas-

<sup>†</sup> Corresponding author. Email: [nppaimit@yahoo.co.in](mailto:nppaimit@yahoo.co.in)

bandy (2007), Ganji and Sadighi (2006), Rafei and Ganji (2006), Rafei et al. (2007), Siddiqui and Irum (2008) ).

By observing the above literature about this type of study, we got motivated to study the characteristic of MHD flow and heat transfer of laminar flow between porous disks through HPM. The main advantage is that it yields a very rapid convergence of the series solution, only with the few iterations. For simple domains the HPM has advantages over pure numerical results. A single computer program gives the solution for a large range of expansion quantity. The steady state solutions of the Navier-Stokes equations are usually obtained by numerical schemes like finite difference or finite element scheme. The numerical methods are difficult to implement due to non-linearity of the equations, so semi-analytical methods are useful in analysing such problems but in the present study both the methods are implemented efficiently in analysing the problem.

## 2. PROBLEM FORMULATION

The problem of the steady laminar flow of an in-compressible viscous fluid between parallel circular non-conducting disks in the presence of a uniform strong magnetic field is investigated for small Reynolds number. The flow under consideration is entirely due to either uniform suction or injection at the disks as shown bellow figure

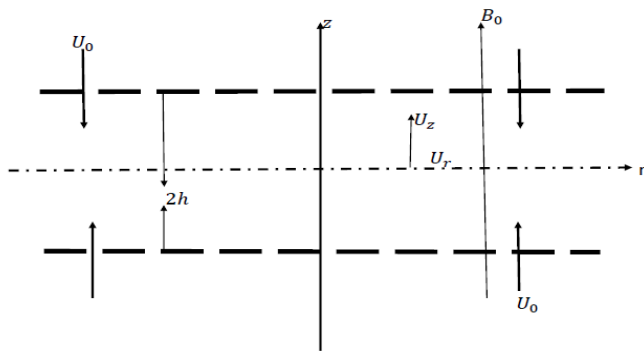


Fig. 1 Geometry of the problem

The governing equations of motion are

$$U_r \frac{\partial U_r}{\partial r} + \frac{U_z}{h} \frac{\partial U_r}{\partial \eta} = -\frac{1}{\rho} \frac{\partial p}{\partial r} + \nu \left[ \frac{\partial^2 U_r}{\partial r^2} + \frac{1}{r} \frac{\partial u_r}{\partial r} - \frac{U_r}{r} + \frac{1}{h^2} \frac{\partial^2 U_r}{\partial \eta^2} \right] - \frac{\mu^2 \sigma H_0^2}{\rho} U_r \quad (1)$$

$$U_r \frac{\partial U_z}{\partial r} + \frac{U_z}{h} \frac{\partial U_z}{\partial \eta} = -\frac{1}{\rho h} \frac{\partial p}{\partial \eta} + \nu \left[ \frac{\partial^2 U_z}{\partial r^2} + \frac{1}{r} \frac{\partial U_z}{\partial r} + \frac{1}{h^2} \frac{\partial^2 U_z}{\partial \eta^2} \right] \quad (2)$$

$$\frac{\partial U_r}{\partial r} + \frac{U_r}{r} + \frac{1}{h} \frac{\partial U_z}{\partial \eta} = 0 \quad (3)$$

The induced magnetic field is assumed to be small and it can be calculated, assuming the velocity  $U_r$  known, from the Maxwell-Ampere's equation:

$$\frac{\partial^2 h r}{\partial \eta^2} + \alpha \mu \sigma h \frac{\partial U_r}{\partial \eta} = 0 \quad (4)$$

The boundary condition on  $h_r$ , if the disks are non-conducting, is

$$h_r = 0 \quad \text{at the disks} \quad (5)$$

The boundary conditions on  $U_r$  and  $U_z$  are the no-slip conditions:

$$U_r(r, \pm h) = 0 \quad (6)$$

and

$$U_z(r, \pm h) = \mp U_0 = \text{constant} \quad (7)$$

The equation for the temperature field, neglecting the viscous dissipation, can be written as

$$\rho c_p \left( u \frac{\partial T}{\partial r} + \frac{w}{a} \frac{\partial T}{\partial \eta} \right) - k_0 \left( \frac{1}{a^2} \frac{\partial^2 T}{\partial \eta^2} + \frac{\partial^2 T}{\partial r^2} + \frac{1}{r} \frac{\partial T}{\partial r} \right) = 0 \quad (8)$$

The boundary conditions for the temperature field can be written as

$$T = \begin{cases} T_1, & \eta = -1 \\ T_2, & \eta = 1 \end{cases} \quad (9)$$

Using the transformation

$$\Phi(r, \eta) = \frac{U_0 r^2}{2} f(\eta) \quad (10)$$

$$\theta(\eta) = \frac{T - T_1}{T_2 - T_1} \quad (11)$$

such that

$$U_r = \frac{1}{rh} \frac{\partial \Phi}{\partial \eta} = \frac{U_0 r}{2h} f'(\eta) \quad (12)$$

and

$$U_z = -\frac{1}{r} \frac{\partial \Phi}{\partial r} = -U_0 f(\eta). \quad (13)$$

Equations (1) and (2), using Eq. (9) and Eq. (10), becomes

$$\frac{U_0 r}{2h} \left[ \frac{U_0}{2h} f'(\eta)^2 - \frac{U_0}{h} f f'' - \frac{\nu}{h^2} f''' + \frac{\mu^2 \sigma H_0^2}{\rho} f' \right] = -\frac{1}{\rho} \frac{\partial p}{\partial r} \quad (14)$$

and

$$\frac{U_0^2}{h} f f' + \frac{\nu U_0}{h^2} f'' = -\frac{1}{\rho h} \frac{\partial p}{\partial \eta}. \quad (15)$$

Since the right hand side of Eq. (12) is a function of  $\eta$  only, it follows that:

$$\frac{\partial^2 p}{\partial r \partial \eta} = 0. \quad (16)$$

Hence, Eq.(11), using Eq. (13), becomes

$$\frac{U_0 r}{2h} \frac{\partial}{\partial \eta} \left[ \frac{U_0}{2h} f'(\eta)^2 - \frac{U_0}{h} f f'' - \frac{\nu}{h^2} f''' + \frac{\mu^2 \sigma H_0^2}{\rho} f' \right] = 0. \quad (17)$$

Equation (14) is true for all  $r$ , if

$$f'''(\eta) + R(f(\eta)f''(\eta) - \frac{1}{2}f'(\eta)^2) - M^2 f'(\eta) = A \quad (18)$$

$$\theta''(\eta) + RPr f(\eta)\theta'(\eta) = 0 \quad (19)$$

The boundary conditions on  $f(\eta)$  and  $\theta(\eta)$  are

$$f(\pm 1) = \pm 1, \quad f'(\pm 1) = 0 \quad (20)$$

$$\theta(-1) = 0, \quad \theta(1) = 1. \quad (21)$$

## 3. METHOD OF SOLUTION

We adopt two methods to solve the problems considered.

**Method-I:** Homotopy Perturbation Solution:

To describe the HPM solution for the system of non-linear differential equations, we consider

$$D_1[f(\eta)] - f_1(\eta) = 0 \quad (22)$$

$$D_2[\theta(\eta)] - f_2(\eta) = 0 \quad (23)$$

where  $D_1$  and  $D_2$  denotes the operator,  $f(\eta)$  and  $\theta(\eta)$  are unknown functions,  $\eta$  denote the independent variable and  $f_1, f_2$  are known functions.  $D_1$  and  $D_2$  can be written as

$$D_1 = L_1 + N_1$$

$$D_2 = L_2 + N_2$$

where  $L_1$  and  $L_2$  are simple linear part,  $N_1$  and  $N_2$  are remaining part of the Eqs. (22) and (23) respectively. The proper selection of  $L_1, L_2, N_1,$  and  $N_2$  form the governing equations one can get the homotopy equation for Eq. (22) and Eq. (23) as follows

$$H1(\Phi_1(\eta, q; q)) = (1 - q)[L1(\Phi_1, q) - L1(v_0(\eta))] + q[D1(\Phi_1, q) - f_1(\eta)] = 0 \quad (24)$$

$$H2(\Phi_2(\eta, q; q)) = (1 - q)[L2(\Phi_2, q) - L2(v_0(\eta))] + q[D2(\Phi_2, q) - f_2(\eta)] = 0 \quad (25)$$

where  $v_0(\eta)$  is the initial guess to the Eq. (22) and Eq. (23). We assume the solution of Eq. (24) and Eq. (25) as follows

$$\Phi_1(\eta, q) = \sum_{n=0}^{\infty} q^n f_n(\eta) \quad (26)$$

$$\Phi_2(\eta, q) = \sum_{n=0}^{\infty} q^n \theta_n(\eta) \quad (27)$$

The solution to the considered problems is Eq. (26) and Eq. (27) at  $q = 1$ . The slow convergence of the above series Eqs. (26) and (27) at  $q = 1$  requires large number of terms for obtaining an almost exact solution. As we proceed for higher approximations, the computations becomes cumbersome and is difficult to calculate the terms manually. So Mathematica software is used to get higher order terms.

By proper selection of linear and non-linear part and applying HPM to solve the consider equations one can get the zeroth and first order solution as follows

$$f_0 = \frac{1}{2}(3\eta - \eta^3)$$

$$f_1 = \frac{1}{560}(-14M^2\eta + 19R\eta + 28M^2\eta^3 - 39R\eta^3 - 14M^2\eta^5 + 21R\eta^5 - R\eta^7)$$

$$f_2 = \frac{1}{2587200} \left( 3388M^4\eta - 2310M^2R\eta - 3288R^2\eta - 8316M^4\eta^3 + 13244M^2R\eta^3 - 2215R^2\eta^3 + 6468M^4\eta^5 - 20328M^2R\eta^5 + 15708R^2\eta^5 - 1540M^4\eta^7 + 10164M^2R\eta^7 - 11682R^2\eta^7 - 770M^2R\eta^9 + 1540R^2\eta^9 - 63R^2\eta^{11} \right)$$

$$\theta_0 = \frac{1}{2}(1 + \eta)$$

$$\theta_1 = \frac{1}{80} \left( 9PrR\eta - 10Pr\eta^3 + PrR\eta^5 \right)$$

$$\theta_2 = \frac{1}{403200} \left( -456M^2PrR\eta + 613PrR^2\eta + 1391P^2R^2\eta + 840M^2PrR\eta^3 - 1140PrR^2\eta^3 - 11340PrR^2\eta^3 - 504M^2PrR\eta^5 + 702PrR^2\eta^5 + 12474Pr^2R^2\eta^5 + 120M^2PrR\eta^7 - 180PrR^2\eta^7 - 2700Pr^2R^2\eta^7 + 5PrR^2\eta^9 + 175Pr^2R^2\eta^9 \right)$$

**Method-II: Finite Difference Solutions:**

The equations mentioned above Eqs. (18, 19) subjected Eqs. (20, 21) were solved numerically by FDM to confirm the results obtained by us. Using standard finite difference method, i.e stepping from  $\eta_{j-1}$  to  $\eta_j$ , a Crank-Nicolson's scheme was used. These tridiagonal systems are easily solved to update the values on each grid point. Calculations were performed by dividing the interval into  $10^4$  sub intervals to find the associated parameters. These system of equations were solved using Mathematica.

**4. RESULT AND DISCUSSION**

The intention of the authors in this study is to analyse the flow and heat transfer characteristics associated with laminar flow between porous disks in the presence of a uniform magnetic field through semi-numerical technique. In this section we illustrate the numerical and semi-numerical findings in graphical and tabular forms with the interpretations and discussion. To develop better understanding of the conducting fluid between two parallel porous disks and thermal characteristics, we choose to present the shear stress, velocity and temperature across the disks for a range of the Reynolds number  $R$ , the magnetic parameter  $M$  and the Prandl number  $Pr$ . The results presented using homotopy perturbation series method by considering 20 terms in the series and also compared the results obtained by HPM with the classical FDM, by dividing the interval in to 10000 sub-intervals. The algebra becomes cumbersome after certain steps we implement these two methods in mathematica software by writing elegant code.

Figures 2 to 7 represent the dimensionless axial and radial velocity for various values of parameters from various angle. Figures 2 to 4 presents the dimensionless axial velocity, from Fig.2 it is clear that the axial velocity takes its dimensionless value 1, at the upper disk and  $-1$ , at the lower disk with a point of inflection on the central plane  $z = 0$ . The axial velocity  $f(\eta)$  increases throughout from  $-1$  to  $1$  for a given value of  $R$ . Figures 4 to 7 represents the behavior of the radial velocity for various values of parameters. The radial velocity profiles are in parabolic nature for all the values of the parameters. The radial velocity increases in the central plane and near the boundary it fall with an increase in the values of  $R$ .

Figures 8 to 14 represents the variation of the temperature for different values of the parameters  $R, M$  and  $Pr$ . Figs. 8 to 10 shows the variation of  $\theta(\eta)$  with  $R$  with fixed values of  $M$  and  $Pr$ . It is observed from these figures that the temperature is increases in the upper half of the plane and decreases in lower region with increase in  $R$ . In Figs. 10 to 12, we fix the values of  $R, M$  and plotted  $\theta(\eta)$  with the variation in  $Pr$ . In Figs. 13 to 14, we fix  $R, Pr$  and plotted temperature profiles with the variation in magnetic parameter for these two cases. Also we observe the similar situation with slight change in position due to increase in the conductivity in the fluid.

Table 1 and Table 2 show the heat transfer rate ( $\theta'(-1)$ ) and the shear stress( $f''(-1)$ ) respectively. In this section we compared the results obtained by the HPM with the classical FDM technique and tabulated the values and the results are in good agreement. From Table 1 it is clear that the heat transfer rate decreases with increase in  $R$ . As we increase the magnetic parameter, heat transfer rate also increases, however as we increase the Prandtl number heat transfer rate decreases. From the Table 1 it is clear that the shear stress decreases as we increase  $R$  and increases with increasing the magnetic parameter.

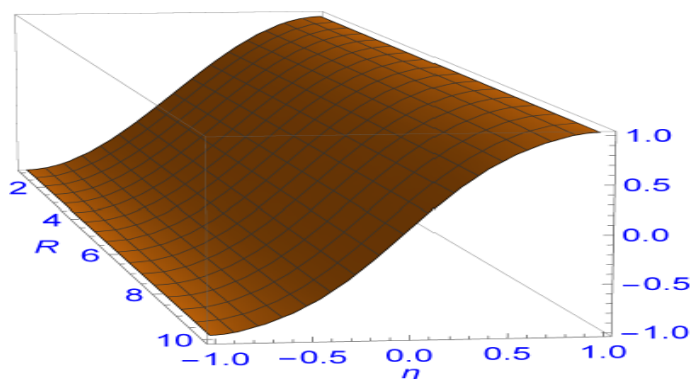


**Fig. 2** Variation of axial velocity with  $R$ , when  $M = 0.2$

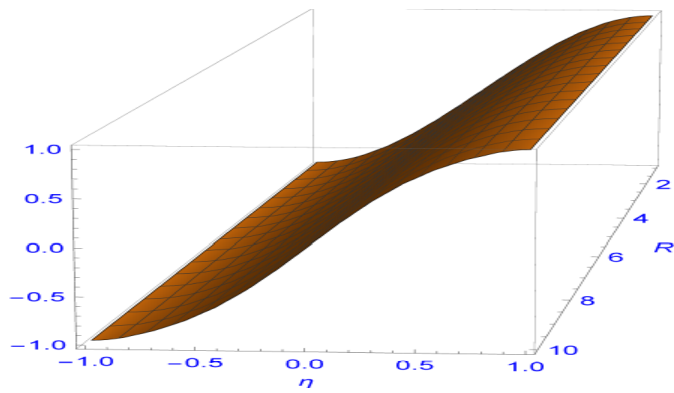


Fig. 3 Variation of axial velocity with  $R$ , when  $M = 0.4$

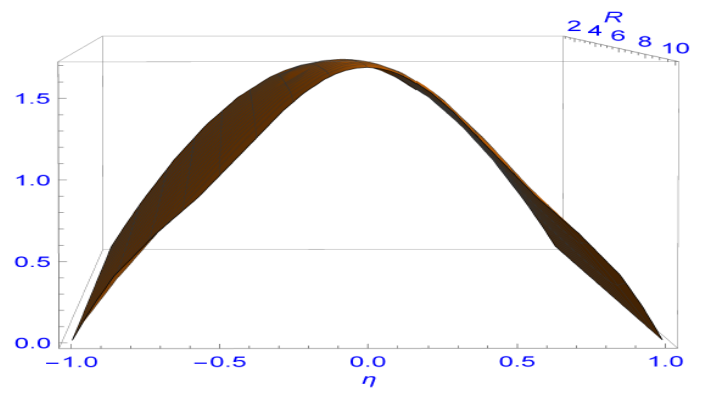


Fig. 7 Variation of radial velocity with  $R$ , when  $M = 0.6$

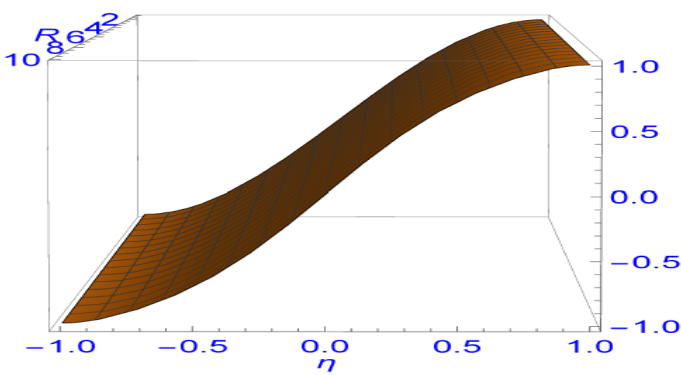


Fig. 4 Variation of axial velocity with  $R$ , when  $M = 0.6$

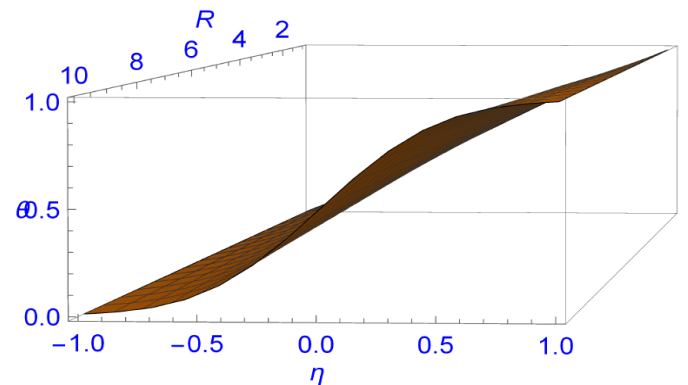


Fig. 8 Temperature variation with  $R$ , when  $M = 0.1$ ,  $Pr = 0.4$

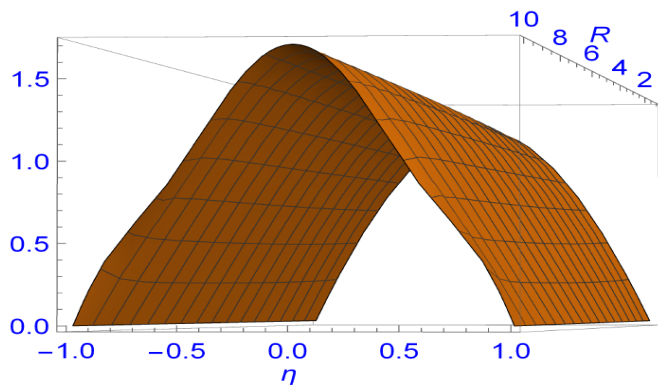


Fig. 5 Variation of radial velocity with  $R$ , when  $M = 0.2$

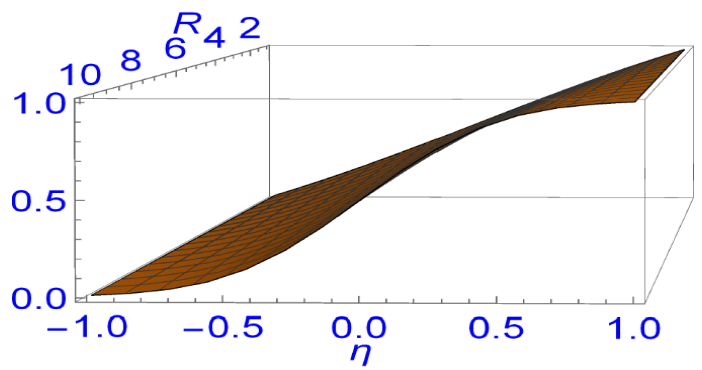


Fig. 9 Temperature variation with  $R$ , when  $M = 0.2$ ,  $Pr = 0.4$

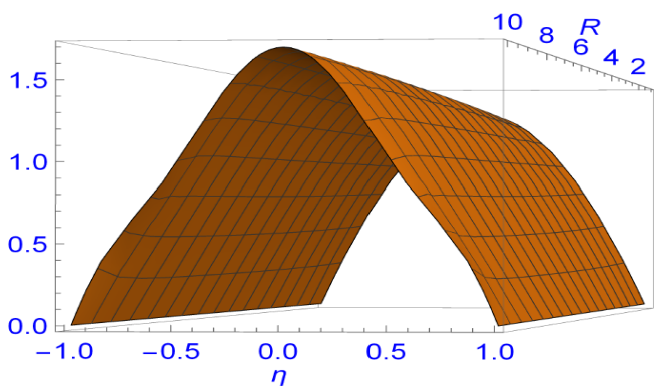


Fig. 6 Variation of radial velocity with  $R$ , when  $M = 0.4$

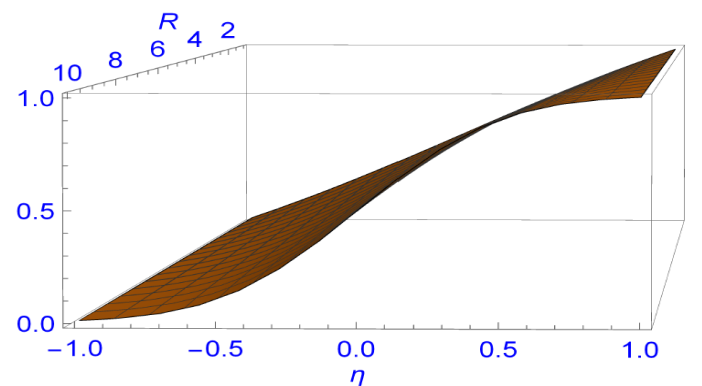


Fig. 10 Temperature variation with  $R$ , when  $M = 0.3$ ,  $Pr = 0.4$

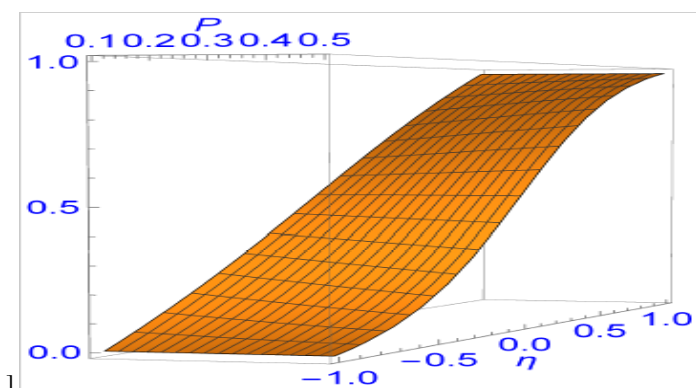


Fig. 11 Temperature variation with  $Pr$ , when  $M = 1.5, R = 5$

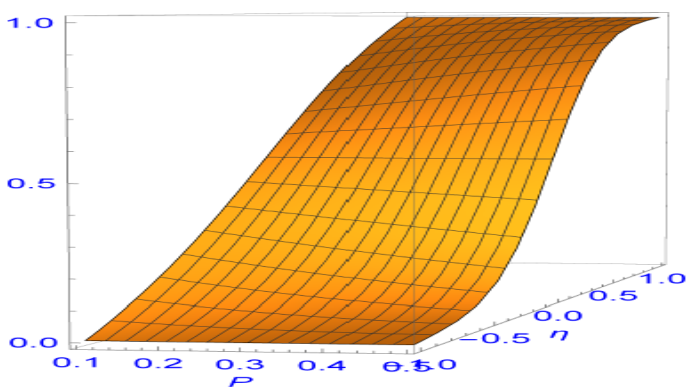


Fig. 12 Temperature variation with  $Pr$ , when  $M = 1.5, R = 10$

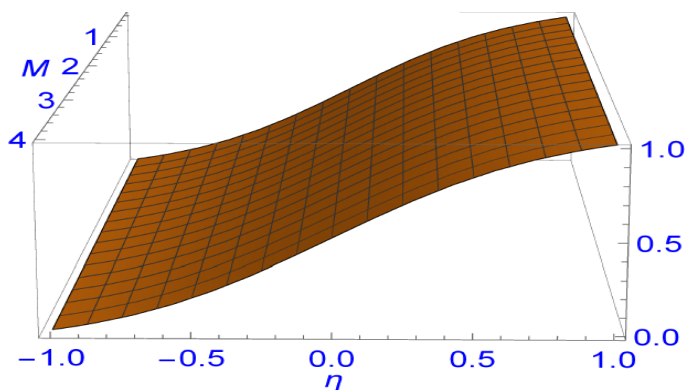


Fig. 13 Temperature variation with  $M$ , when  $Pr = 0.4, R = 5$

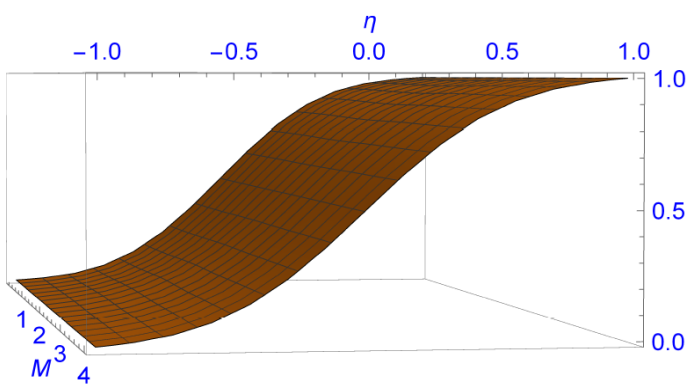


Fig. 14 Temperature variation with  $M$ , when  $Pr = 0.4, R = 10$

Table 1 Values of Nusselt number ( $\theta'(-1)$ ).

R	$Pr$	M	HPM	FDM	M	HPM	FDM
1	0.1	0.2	0.48019	0.480151	0.6	0.48022	0.48018
2			0.46081	0.460777		0.46087	0.46083
3			0.44190	0.441873		0.44198	0.44194
4			0.42350	0.423479		0.42360	0.42357
5			0.40565	0.405625		0.40575	0.40573
6			0.38834	0.38833		0.38846	0.38844
7			0.37160	0.37159		0.37172	0.37171
8			0.35538	0.35541		0.35552	0.35555
9			0.33933	0.339802		0.33958	0.33993
10			0.32072	0.32474		0.32176	0.32488
1	0.1	0.4	0.48021	0.48016	0.8	0.48025	0.48020
2			0.46083	0.46079		0.46091	0.46088
3			0.44193	0.44190		0.44204	0.44201
4			0.42354	0.42351		0.42368	0.42365
5			0.40569	0.40567		0.40584	0.40582
6			0.38839	0.38837		0.38856	0.38854
7			0.37165	0.37164		0.37183	0.37182
8			0.35543	0.35546		0.35564	0.35565
9			0.33942	0.33985		0.33980	0.34005
10			0.32110	0.32480		0.32271	0.322499
1	0.2	0.2	0.46100	0.46097	0.6	0.46106	0.46102
2			0.42406	0.42404		0.42416	0.42414
3			0.38924	0.38923		0.38938	0.38936
4			0.35657	0.35656		0.35674	0.35673
5			0.32604	0.32604		0.32622	0.32623
6			0.29761	0.29762		0.29781	0.29781
7			0.27122	0.27123		0.27142	0.27143
8			0.24671	0.24681		0.24694	0.24701
9			0.22331	0.22426		0.22380	0.22446
10			0.19564	0.20349		0.19810	0.20368
1	0.2	0.4	0.46102	0.46099	0.8	0.46111	0.46107
2			0.42410	0.42407		0.42425	0.42423
3			0.38929	0.38928		0.38950	0.38949
4			0.35663	0.35662		0.35688	0.35688
5			0.32611	0.32611		0.32638	0.32637
6			0.29769	0.29769		0.29797	0.29798
7			0.27129	0.27131		0.27159	0.27160
8			0.24680	0.24689		0.24713	0.24718
9			0.22349	0.22434		0.22421	0.22462
10			0.19656	0.203569		0.20024	0.20385
1	0.3	0.2	0.44242	0.44238	0.6	0.44250	0.44247
2			0.38967	0.38966		0.38982	0.38980
3			0.34174	0.34174		0.34193	0.34192
4			0.29851	0.29852		0.29873	0.29874
5			0.25978	0.25979		0.26001	0.26003
6			0.22529	0.22531		0.22552	0.22554
7			0.19474	0.19477		0.19498	0.19500
8			0.16771	0.16787		0.16799	0.16809
9			0.14281	0.144278		0.14356	0.14448
10			0.11171	0.12368		0.11620	0.12387
1	0.3	0.4	0.44244	0.44241	0.8	0.44257	0.44254
2			0.38973	0.38971		0.38994	0.38993
3			0.34181	0.34181		0.34210	0.34210
4			0.29859	0.29859		0.29892	0.29893
5			0.25987	0.25988		0.26021	0.26021
6			0.22538	0.22540		0.22573	0.22574
7			0.19483	0.19486		0.19518	0.19520
8			0.16782	0.16795		0.16822	0.16828
9			0.14309	0.144356		0.14419	0.14466
10			0.11340	0.12375		0.11998	0.12403

1	0.4	0.2	0.42442	0.42440	0.6	0.42453	0.42450
2			0.35756	0.35756		0.35775	0.35774
3			0.29911	0.29912		0.29934	0.29933
4			0.24857	0.24858		0.24882	0.24883
5			0.20532	0.20533		0.20557	0.20560
6			0.16865	0.16867		0.16890	0.16891
7			0.13782	0.13785		0.13805	0.13808
8			0.11191	0.11214		0.11222	0.11235
9			0.08865	0.09084		0.08980	0.09102
10			0.05570	0.07330		0.06341	0.07346
1	0.4	0.4	0.42446	0.42444	0.8	0.42462	0.42456
2			0.35763	0.35762		0.35790	0.35790
3			0.29919	0.29920		0.29954	0.29954
4			0.24866	0.24867		0.24904	0.24906
5			0.20541	0.20543		0.20580	0.20581
6			0.16874	0.16877		0.16911	0.16913
7			0.13791	0.13794		0.13826	0.13828
8			0.11203	0.11222		0.11248	0.11253
9			0.08908	0.09091		0.09075	0.09118
10			0.05863	0.07336		0.069780	0.07360

**Table 2** Values of shear stress  $f''(-1)$ .

R	M	HPM	FDM	M	HPM	FDM
1	0.2	2.78136	2.78070	0.4	2.80313	2.80240
2		2.60927	2.60908		2.6289	2.62842
3		2.48025	2.48001		2.49785	2.49767
4		2.38413	2.38376		2.39986	2.39937
5		2.31251	2.31218		2.32658	2.32640
6		2.25887	2.25870		2.27149	2.27128
7		2.21892	2.21776		2.23028	2.22946
8		2.19812	2.18666		2.20813	2.19713
9		2.28767	2.16253		2.29358	2.17198
10		3.22869	2.14334		3.20662	2.15209
1	0.6	2.83913	2.83860	0.8	2.88895	2.88840
2		2.66142	2.66092		2.70650	2.70622
3		2.52702	2.52646		2.56754	2.56737
4		2.42597	2.42564		2.46229	2.46220
5		2.34996	2.34994		2.38252	2.38200
6		2.29248	2.29211		2.32176	2.32139
7		2.24916	2.24821		2.27549	2.27473
8		2.22454	2.21438		2.24702	2.23831
9		2.30119	2.18768		2.30792	2.20946
10		3.15457	2.1633		3.05463	2.18648

## 5. CONCLUSIONS

The present study has revealed the effects of governing parameters on the flow in presence of magnetic field and thermal effects. The resulting equations with associate boundary conditions are solved by HPM and finite difference method.

The following conclusions are emerging out of the study:

- 1) The shear stress and heat transfer rate decreases by increasing in injection.
- 2) The heat transfer rate decreases with increase in  $Pr$ .
- 3) The shear stress increases with increase in magnetic parameter.
- 4) The radial velocity increases near central plane with increase in Reynolds number, where as it decreases with increase in magnetic field and they are parabolic in nature.

## NOMENCLATURE

$z, r$	axial and radial coordinates
$U_r$	radial component of velocity
$U_z$	axial component of velocity
$2h$	distance between tow disk
$U_0$	injection velocity
$\eta$	dimensionless axial coordinate, $\frac{z}{h}$
$\rho$	density
$\nu$	coefficient of kinematic viscosity
$\mu$	magnetic permeability
$H_0$	impressed magnetic field
$H_r$	induced magnetic field
$M$	Hartmann number
$R$	Reynolds number

## REFERENCES

- Abbasbandy, S., 2007, "Application of He's homotopy perturbation method to functional integral equations." *Chaos, Solitons and Fractals*, **31**(5), 1243–1247.  
<https://doi.org/10.1016/j.chaos.2005.10.069>.
- Abed, I.M., Ali, H.F., and Sahib, S.A.M., 2020, "Investigation of heat transfer and fluid flow around sinusoidal corrugated circular cylinder for two dimensional system," *Frontiers in Heat and Mass Transfer*, **15**(6), 1–9.  
<http://dx.doi.org/10.5098/hmt.15.6>.
- Batchelor, G.K., 1967, *An Introduction to Fluid Dynamics*, 1st ed., Cambridge University Press, University of Cambridge.
- Bujurke, N.M., Pai, N.P., and Achar, P.K., 1995, "Semi analytical approach to stagnation-point flow between porous plates with mass transfer," *Indian J Pure appl Math*, **4**(26), 373–389.  
<http://dx.doi.org/10.1063/1.2975972>.
- Chandrasekhara, B.C., and Rudriah, N., 1971a, "Magnetohydrodynamic laminar flow between porous disks." *Appl Sci Res*, **23**, 42–52.  
<https://doi.org/10.1007/BF00413186>.
- Chandrasekhara, B.C., and Rudriah, N., 1971b, "Three dimensional MHD flow between two porous disks." *Applied scientific research*, **25**, 179–192.  
<https://doi.org/10.1007/BF00382294>.
- Gadamsetty, R., Sajja, V.S., Sekhar, P.S., and Prasad, D., 2020, "Thermal effects in Bingham plastic fluid film lubrication of asymmetric rollers," *Frontiers in Heat and Mass Transfer*, **15**(18), 1–7.  
<http://dx.doi.org/10.5098/hmt.15.18>.
- Ganji, D., and Sadighi, A., 2006, "Application of He's homotopy perturbation method to nonlinear coupled system of reaction-diffusion equations." *International Journal of Nonlinear sciences and Numerical Simulation*, **7**(4), 411–418.  
<https://doi.org/10.1515/IJNSNS.2006.7.4.411>.
- Gu, X., Jiang, G., Wo, Y., and Chen, B., 2020, "Numerical study on heat transfer characteristics of propylene glycole-water mixture in shell side of spiral wound heat exchanger," *Frontiers in Heat and Mass Transfer*, **15**(3), 1–8.  
<http://dx.doi.org/10.5098/hmt.15.3>.
- Gupta, S., Kumar, D., and Singh, J., 2013, "Application of He's homotopy perturbation method for solving nonlinear wave-like equations with variable coefficients." *International Journal of Advances in Applied Mathematics and Mechanics*, **1**(2), 65–79.  
<http://www.ijaamm.com/uploads/2/1/4/8/21481830/ijaamm-y2013v1n2p6-devendrakumar.pdf>.

- He., J.H., 2006, "New interpretation of homotopy perturbation method." *International Journal of Modern Physics B*, **20**(18), 2561–2568.  
<https://doi.org/10.1142/S0217979206034819>.
- Karman, T.V., 2021, "Uber laminare and turbulente reibung," *Journal of applied mathematics and mechanics*.  
<https://doi.org/10.1002/zamm.19210010401>.
- Lance, G.N., and Rogers, M., 1962, "The axially symmetric flow of a viscous flow between two infinite rotating disks," *Proc Royal Soc London*, **266**(1324), 109–121.  
<https://doi.org/10.1098/rspa.1962.0050>.
- Mellor, G.L., Chapple, P.J., and Stokes, V.K., 1968, "On the flow between a rotating and stationary disk," *Journal of fluid mechanics*, **31**(1), 95–112.  
<https://doi.org/10.1017/S0022112068000054>.
- Nazir, A., and Mahmood, T., 2011, "Analysis of flow and heat transfer of viscous fluid between contracting rotating disks," *Applied mathematical modelling*, **35**(7), 3154–3165.  
<https://doi.org/10.1016/j.apm.2010.12.015>.
- Osalus, E., Side, J.C., and Harris, R.E., 2007, "Effects of Ohmic heating and viscous dissipation on unsteady MHD and slip flow over a porous rotating disk with variable properties in the presence of Hall and ion-slip currents," *International Communications in Heat and Mass Transfer*, **34**(9-10), 1017–1029.  
[10.1016/j.icheatmasstransfer.2007.05.009](https://doi.org/10.1016/j.icheatmasstransfer.2007.05.009).
- Rafei, M., and Ganji, D.D., 2006, "Explicit solutions of Helmholtz equation and fifth-order Kdv equation using homotopy perturbation method ." *International Journal of Nonlinear sciences and Numerical Simulation*, **7**(3), 321–328.  
<https://doi.org/10.1515/IJNSNS.2006.7.3.321>.
- Rafei, M., Ganji, D.D., and Daniali, D., 2007, "Solution of epidemic model by homotopy perturbation method ." *Applied mathematics and computation*, **187**(2), 1056–1062.  
<https://doi.org/10.1016/j.amc.2006.09.019>.
- Raju, A., Ojjela, O., Kumar, N.N., and Munjam, S.R., 2019, "Heat and mass transfer analysis of MHD couple stress fluid flow through expanding or contracting porous pipe with cross diffusion effects," *International journal of dynamics and control*, **7**(3), 1293–1305.  
<https://doi.org/10.1007/s40435-019-00545-6>.
- Root, N., and Lewellen, W.S., 1966, "Flow between a rotating stationary disk," *Prog Aero Sci*, **7**, 136.
- Sampath, V.S.K., and Pai, N., 2019a, "A study of magnetic effect on flow between two plates with suction or injection with special reference to casson fluid," *Multidiscipline Modeling in Materials and Structures*, **15**(3), 559–574.  
<https://doi.org/10.1108/MMMS-05-2018-0092>.
- Sampath, V.S., and Pai, N., 2019b, "A study of magnetic effect on flow between two plates with suction or injection with special reference to casson fluid," *Frontiers in Heat and Mass Transfer*, **12**(23), 1–9.  
<http://dx.doi.org/10.5098/hmt.12.23>.
- Sibanda, P., and Makinde, O.D., 2012, "On steady MHD flow and heat transfer past a rotating disk in a porous medium with ohmic heating and viscous dissipation," *International journal of numerical methods for heat and fluid flow*, **20**(3), 269–285.  
<https://doi.org/10.1108/09615531011024039>.
- Siddiqui, A., and Irum, S., 2008, "Unsteady squeezing flow of a viscous mhd fluid between parallel plates, a solution using the homotopy perturbation method." *Mathematical Modelling and Analysis*, **13**(4), 565–576.  
<https://doi.org/10.3846/1392-6292.2008.13.565-576>.
- Srivastava, A.C., and Sharma, S.K., 1961, "The effect of a transverse magnetic field on the flow between two infinite disks," *Bull Acad Pol Sci*, **9**, 639–644.  
<https://www.osti.gov/etdeweb/biblio/7298242>.
- Stephenson, C.J., 1969, "Magnetohydrodynamic flow between rotating-coaxial disks," *Journal of Fluid Mechanics*, **38**(2), 335–352.  
<https://doi.org/10.1017/S0022112069000206>.
- Stewartson, K., 1953, "On the flow between two rotating coaxial disks," *Proc Camb Phil Soc*, **49**, 533.  
<http://dx.doi.org/10.1063/1.2975972>.
- Tufail, M.N., Saleem, M., and Chaudhry, Q.A., 2020, "Heat transfer analysis for the unsteady UCM fluid flow with hall effects: The two parameter lie transformations," *Frontiers in Heat and Mass Transfer*, **15**(14), 1–10.  
<http://dx.doi.org/10.5098/hmt.15.14>.
- Wang, C.Y., and Watson, L.T., 1979, "Viscous flow between rotating discs with injection on the porous disc," *Journal of Applied Mathematics and Physics*, **30**, 773–787.  
<https://doi.org/10.1007/BF01590686>.
- Xinhui, S., Liancum, Z., Xinxin, Z., and Xinyi, S., 2012, "Homotopy analysis method for the asymmetric laminar flow and heat transfer of viscous fluid between contracting rotating disks," *Applied Mathematical Modelling*, **36**(4), 1806–1820.  
<https://doi.org/10.1016/j.apm.2011.09.010>.